

## Accepted Manuscript

Phylogeographic structure of *Canthon cyanellus* (Coleoptera: Scarabaeidae), a Neotropical dung beetle in the Mexican Transition Zone: insights on its origin and the impacts of Pleistocene climatic fluctuations on population dynamics

Janet Nolasco-Soto, Jorge González-Astorga, Alejandro Espinosa de los Monteros, Eduardo Galante-Patiño, Mario E. Favila

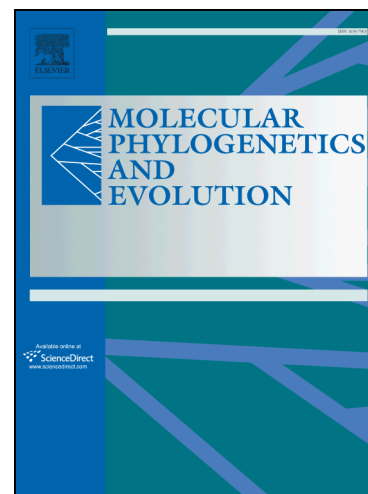
PII: S1055-7903(17)30014-3  
DOI: <http://dx.doi.org/10.1016/j.ympev.2017.01.004>  
Reference: YMPEV 5724

To appear in: *Molecular Phylogenetics and Evolution*

Received Date: 2 May 2016  
Revised Date: 16 December 2016  
Accepted Date: 6 January 2017

Please cite this article as: Nolasco-Soto, J., González-Astorga, J., Espinosa de los Monteros, A., Galante-Patiño, E., Favila, M.E., Phylogeographic structure of *Canthon cyanellus* (Coleoptera: Scarabaeidae), a Neotropical dung beetle in the Mexican Transition Zone: insights on its origin and the impacts of Pleistocene climatic fluctuations on population dynamics, *Molecular Phylogenetics and Evolution* (2017), doi: <http://dx.doi.org/10.1016/j.ympev.2017.01.004>

This is a PDF file of an unedited manuscript that has been accepted for publication. As a service to our customers we are providing this early version of the manuscript. The manuscript will undergo copyediting, typesetting, and review of the resulting proof before it is published in its final form. Please note that during the production process errors may be discovered which could affect the content, and all legal disclaimers that apply to the journal pertain.



**Phylogeographic structure of *Canthon cyanellus* (Coleoptera: Scarabaeidae), a Neotropical dung beetle in the Mexican Transition Zone: insights on its origin and the impacts of Pleistocene climatic fluctuations on population dynamics**

**Janet Nolasco-Soto<sup>1\*</sup>, Jorge González-Astorga<sup>2</sup>, Alejandro Espinosa de los Monteros<sup>1</sup>, Eduardo Galante-Patiño<sup>3</sup>, Mario E. Favila<sup>4</sup>**

<sup>1</sup>Laboratorio de Sistemática Filogenética, Red de Biología Evolutiva, Instituto de Ecología, A.C. Carretera Antigua a Coatepec No. 351, Xalapa 91070, Veracruz, Mexico.

<sup>2</sup>Laboratorio de Genética de Poblaciones, Red de Biología Evolutiva, Instituto de Ecología, A.C. Carretera Antigua a Coatepec No. 351, Xalapa 91070, Veracruz, Mexico.

<sup>3</sup>Centro Iberoamericano de la Biodiversidad (CIBIO), Universidad de Alicante, Carretera de San Vicente del Raspeig s/n 03690 San Vicente del Raspeig, Alicante, Spain.

<sup>4</sup>Red de Ecoetología, Instituto de Ecología, A.C. Carretera Antigua a Coatepec No. 351, Xalapa 91070, Veracruz, Mexico.

\*Correspondence author: [janet.nolasco@inecol.mx](mailto:janet.nolasco@inecol.mx)

**Abstract**

*Canthon cyanellus* is a roller dung beetle with a wide distribution range in the tropical forests of the New World. In Mexico, it inhabits the Pacific and the Gulf coasts, the Yucatan Peninsula and the south mainly in the State of Chiapas. This species shows a wide geographical variation in cuticle color, which has been used as defining trait for subspecies. In this study we analyzed the phylogeographic and demographic history of the Mexican populations of *C. cyanellus* using DNA sequences of the nuclear *ITS2*, and the mitochondrial *COI* and *16S* genes. We found that not all the current valid subspecies are supported by the molecular analysis. The populations are genetically and geographically structured in five lineages. The diversification events that gave origin to the main lineages within this species complex occurred during the Pleistocene in a time range of 1.63 to 0.91 Myr. The demographic history of these lineages suggests post-glacial expansions toward the middle and the end of the Pleistocene. The combined data of mitochondrial and nuclear DNA suggest that the phylogeographic structure and demographic history of the *C. cyanellus* populations are the result of: the geological and volcanic activity that occurred from the end of the Pliocene to the Pleistocene; and the contraction and expansion of tropical forests due to the glacial and inter-glacial cycles during the Pleistocene. Landscape changes derived from historical events have affected the demographic history of the populations of this species. The results presented here point to the need to review the taxonomic status and delimitation of the lineages encompassed in the *Canthon cyanellus* complex.

**Key words**

Historical demography, Mexico, Neotropics, Population divergence, Pleistocene glaciations

## 1. Introduction

The area of confluence between the Nearctic and the Neotropical regions is known as the Mexican Transition Zone (MTZ), which has fostered the *in-situ* or vicariant allopatric differentiation of a number of insect groups (Halffter, 1976). The MTZ is a major corridor/barrier that has driven the geographic distribution of several taxa, from plants to insects. In particular Mexico's Neotropical entomofauna shows phylogenetic affinities with South American insects (Halffter, 1976, 1987). Retrieving the phylogeographic processes associated to dispersion and vicariance allows one to better understand the evolution of the taxa in terms of historical patterns.

The tribe Deltochilini Lacordaire, 1856 (Scarabaeidae: Scarabaeinae) (formerly Canthonini, Tarasov and Génier, 2015) is one of the most diverse Neotropical Scarabaeinae tribes (Davis et al., 2008). Within the tribe, the genus *Canthon* is the most species rich lineage encompassing 174 species (Halffter and Martínez, 1977). The genera within this tribe expanded from South America to Central and North America during two possible expansion events (Halffter, 1976). One occurred before or during the Miocene, and another from the Plio-Pleistocene to date. Beetles within *Canthon*, *Melanocanthon*, *Boreocanthon* and *Glaphyrocانthon*, are examples of those expansion events (Kohlmann and Halffter, 1990).

Kohlmann and Halffter (1990) suggest that beetle representatives of the ancient invasion are currently distributed in biomes that originated in the Miocene (i.e., arid zones, grasslands, and temperate deciduous forests in North America). *Canthon cyanellus*, *C. indigaceus* and *C. morsei* are lines of recent origin distributed in biomes that developed during the Plio-Pleistocene in tropical rainforests; as well as species in *Glaphyrocانthon*, which invaded North America from South America through the southern lowlands of Mexico along the Pacific and Gulf of Mexico slopes, producing a distribution pattern known as 'Typical Neotropical' (Morrone, 2015).

*Canthon cyanellus* LeConte (1859) is a Neotropical roller dung beetle. Kolhmann and Halffter (1990) suggested that this species might have originated in Central or South American during the Plio-Pleistocene period. This species shows high phenotypic variation mainly in cuticular coloration, which can range from largely reddish brown to entirely green or blue. It is distributed from Texas, to Ecuador (Solís and Kohlmann, 2002). Robinson (1948) stated that the southernmost distribution of *C. cyanellus* in the New World is located in Brazil and Peru. Based on Robinson's proposal (1948), Halffter (1961) placed the different chromatic morphs within a single species (*C. cyanellus*), recognizing three subspecies that can be distinguished mostly by differences in color. The subspecies *C. c. cyanellus* (LeConte 1859) has blue- and green-colored morphs with reddish brown parts largely missing. In this subspecies the pygidium has the same coloration as the rest of the body. Its known distribution range encompasses Texas and Mexico in the states of Nuevo Leon, San Luis Potosi, Hidalgo, Morelos, Guerrero, Veracruz, Tabasco, Yucatan and Quintana Roo (Halffter, 1961). *Canthon c. sallei* has the dorsal surface largely reddish brown with various greenish tones, the elytra are reddish brown with greenish black markings, and the disc of the pronotum is largely light reddish or yellowish brown. This subspecies is distributed in Guatemala, Honduras, Costa Rica, Panama, Colombia, Peru and Nicaragua; however it has recently been found in southern Mexico (Favila, unpublished data). *Canthon c. violetae* differs in the color of the pronotum and pygidium, which are largely reddish brown. It is endemic to southern Mexico.

Solís and Kohlmann (2002) studied the genus *Canthon* in Costa Rica and noted that the same locality host the different morphs that define the three subspecies. Some of the Costa Rican morphs show cuticle coloration almost identical to that of *C. c. cyanellus* from Mexico, but always have a yellow pygidium, whereas the populations in Nicaragua and Honduras have the light body coloration of *C. c. sallei*, whose coloration patterns reoccur in South America.

Ortiz-Domínguez et al. (2006), working with *C. c. cyanellus*, analyzed the sexual recognition between sexes of the same population and those of different populations along a latitudinal gradient of the Gulf of Mexico slope. Their results indicate that populations geographically separated by  $\geq 600$  km are undergoing an speciation process as they differ in their sexual recognition mechanisms, as well as differences in cuticle hydrocarbons, which are important for sexual recognition, and a low reproductive success. Nonetheless, under laboratory conditions the individuals maintain reproductive compatibility. Therefore, studies comparing more populations are needed to determine whether this species is still cohesive or if it is a complex of cryptic species. Hence, various genetically and geographically differentiated lineages would be expected in this species, as has been found in some phylogeographic studies for other taxa (Breeschoten et al., 2016; Guevara-Chumacero et al., 2010; Leaché et al., 2013; Maldonado-Sánchez et al., 2016; Pringle et al., 2012; Suárez-Atilano et al., 2014).

To identify the evolutionary and historical processes that have led to the diversification and current distribution of *Canthon cyanellus* in Mexico, we set the following objectives: (1) to infer its genetic diversity and population structure; (2) to determine whether it includes genetically and geographically distinct lineages; (3) to elucidate its demographic history; and (4) to determine whether climatic fluctuations in the Pleistocene had any effect on the diversification and historical demography of this species in Mexico.

## 2. Materials and Methods

### 2.1. Sample collection, DNA extraction and sequencing

A total of 97 individuals were collected and sequenced from ten localities in Mexico. These are situated at the Pacific and the Gulf of Mexico slopes, and the Sierra Madre Oriental (Table 1 and Fig. 1). Those populations were selected because they encompass all the phenotypic variation

described in the subspecies. All biological material was transported alive to the laboratory and subsequently frozen at  $-70^{\circ}\text{C}$ .

We used sequences of the nuclear Internal Transcribed Spacer Region 2 (*ITS2*), and of two mitochondrial genes: Cytochrome Oxidase Subunit I (*COI*) and *16S* rRNA. DNA was obtained by grinding both hind legs of each beetle which were processed according to the protocol of the DNeasy Blood & Tissue kit (QIAGEN). The *COI* gene was amplified with primers M202 “Jerry” (5'-caacattatgtttgatttttgg-3') and M70 “Pat” (5'-tccaatgcactaatctgcatatta-3') (Simon et al., 1994). For *16S* we used the primers M14 “16Sar” (5'-cgctgtttaacaaaaacat-3') and M233 “ND1A” (5'-ggtccttacgaattgaatatact-3') (Simon et al., 1994). *ITS2* was amplified with *ITS2A* (5'-tgtgaactgcaggacacat-3') and *ITS2B* (5'-tatgcttaaattcaggggt-3') (Beebe and Saul, 1995).

PCRs were run in a 25  $\mu\text{l}$  volume: 1  $\mu\text{l}$  DNA (20-40 ng), 4  $\mu\text{l}$  5X Buffer, 2  $\mu\text{l}$   $\text{MgCl}_2$  (25mM), 2.5  $\mu\text{l}$  dNTPs (8  $\mu\text{M}$ ), 0.25  $\mu\text{l}$  BSA, 0.8  $\mu\text{l}$  of each primer (10  $\mu\text{M}$ ), 0.2  $\mu\text{l}$  Taq polymerase (5 U/ $\mu\text{l}$ ) and 13.35  $\mu\text{l}$  ddH<sub>2</sub>O. PCR conditions were as follows: initial denature at 94  $^{\circ}\text{C}$  for 3 min, followed by 30 cycles at 94  $^{\circ}\text{C}$  for 1 min for denaturing, 50  $^{\circ}\text{C}$  for 1 min for annealing, and 70  $^{\circ}\text{C}$  as extension temperature for 2 min, finishing with an extension step at 72  $^{\circ}\text{C}$  for 5 min. Slight variations of this protocol were used for specific fragments. The best yield for *16S* was obtained with 35 cycles, whereas for *ITS2* the optimal annealing was at 53  $^{\circ}\text{C}$ .

PCR products were visualized on 1% agarose gels stained with ethidium bromide, and purified with the QIAquick kit (QIAGEN). Purifications were sent for sequencing in both directions to Macrogen (South Korea). Sequences were edited with Sequencher v5 (Gene Codes Corp, Ann Arbor, Michigan) and aligned with BioEdit v7.0.9 (Hall, 1999). The default options set were used to produce the best alignment. Subsequently, this alignment was refined manually with Mesquite v3.1 (Maddison and Madisson, 2010).

## 2.2. Geographic structure and Genetic diversity

A spatial analysis of molecular variance (SAMOVA) was carried out to identify genetic congruent geographic regions. This analysis was done with the aid of SAMOVA v1 (Dupanloup et al., 2002) using 100 annealing steps to obtain the fixation index ( $F_{CT}$ ; Excoffier et al., 1992). This analysis was performed on the combined data set (*ITS2+16S+COI*) in order to identify the number of groups (K) that are statistically significant. A non-hierarchical analysis of molecular variance (AMOVA) was performed including all the populations, followed by a hierarchical analysis among the statistically significant regions identified by the SAMOVA. These analyses were conducted for each locus with 1000 permutations using Arlequin v3.5 (Excoffier and Lischer 2010). A Mantel test (Mantel, 1967), based on the combined data set, was applied to test for correlation between genetic and geographic distance matrices. For this test the Ade4 package (Chessel et al., 2004) for R was used with 999 replicates. The genetic distance matrix was estimated using MEGA v7 (Kumar et al., 2016) applying the Maximum Composite Likelihood method, excluding gaps and bootstrapping for 500 replicates.

For each locus, the nucleotide ( $\pi$ ) and haplotype (Hd) diversity (Nei, 1987) were estimated using DnaSP v5.10 (Librado and Rozas, 2009). This analysis was conducted for each population, as well as for each of the regions inferred in the SAMOVA. Haplotype networks were constructed with Network v4.5 (Bandelt et al., 1999) using the median-joining algorithm.

## 2.3. Genealogical reconstruction

We approached the study by recognizing evolutionary units based on the phylogenetic species concept (De Queiroz, 2007). Genealogies were inferred for the nDNA data set (*ITS2*), mtDNA data set (*COI+16S*) and combined data set (*ITS2+COI+16S*). Homologous sequences from closely related species (i.e., *Canthidium centrale*, *Canthon viridis*, *C. luteicollis* and *C.*



*smaragdulus*) were used as outgroup. Genealogies were estimated with a Bayesian inference analysis (BI) using MrBayes v3.2.3 (Ronquist et al., 2012) on the CIPRES portal (Miller et al., 2010). The nucleotide substitution model for each locus was selected using the Akaike information criterion (Alfaro and Huelsenbeck, 2006) in jMODELTEST v2.0.2 (Posada, 2008). Ten million replicates were used for the nDNA, 20 million for the mtDNA and 40 million for the combined data set. In each case, trees and parameters were sampled every 1000 generations. The majority-rule consensus tree was obtained, with their respective posterior probabilities (PP), after discarding the initial 25% of the accumulated trees (Ronquist et al., 2012). Neighbor-joining analyses were carried out to contrast the results from the BI analyses. Neighbor-joining trees were constructed with the aid of the software MEGA v7 (Kumar et al., 2016). The detailed methods and results from these analyses can be consulted in Supplementary material S3.

#### 2.4. Divergence times and Historical demography

For dating and inferring potential isolation events in the populations of *C. cyanellus*, we used the software BEAST v1.8.2 (Drummond et al., 2012). As a tree prior for optimizing the genealogy, the BI topology inferred from the combined data set was used. To estimate divergence times, the 'relaxed clock' model was used. The genealogy was calibrated using the nucleotide substitution rates of 0.85% per million years estimated for *ITS2* (Caccone et al., 1988), 1.2% for *16S rRNA* and 2% for *COI* (Papadopoulou et al., 2010).

The nucleotide substitution models, as well as the parameters used as priors for each locus, were those indicated by jMODELTEST. The coalescence process was used as prior for the tree model. Monte Carlo Markovian Chains (MCMC) were run for 20 million generations, sampling trees and parameters every 1000 generations. Analysis consisted of two independent

runs with one cold and three hot chains. The program TRACER v1.6 (Rambaut et al., 2014) was used for assessing stationarity of the MCMC, effective sample sizes (ESSs > 200), and posterior intervals spanning the 95% highest posterior density. These analyzes were repeated four times and the resulting trees from each run were combined using LogCombiner v1.8.2, applying a burn-in of 25%. The nodes evaluated were those that had a PP value > 80%. The inferred chronogram was displayed with the program FigTree v1.4.2 (Rambaut, 2008).

To determine the historical demographic dynamics of the populations, Fu's  $F_s$  neutrality test (Fu, 1997) was performed. The historical demography was compared and visualized with the generalized Skyline-plot analysis using the software BEAST v1.8.2 (Drummond et al., 2012). The parameters used as priors, as well as the molecular clock model, were identical to those used for the coalescence analyses for node dating. Skyline-plots were drawn for the major lineages inferred from the BI analysis (combined data set) and for the ingroup as a whole.

### 2.5. *Dispersal versus vicariance processes*

To infer the dispersal and vicariance events occurring during the evolutionary history of *Canthon cyanellus*, we used the statistical dispersal-vicariance analysis (S-DIVA) as implemented in the software RASP v2.1 beta (Yu et al., 2010, 2013). The ancestral states of each node in the condensed tree were reconstructed using the 75% remaining trees (i.e., 79,996 trees after 'burn-in') generated in BEAST. RASP reconstruction provides estimates of the probability of the ancestral areas at each node, taking into account phylogenetic uncertainty (Nylander et al., 2008). Six geographical regions were defined for the ingroup according to the SAMOVA results [i.e., Gomez Farias (*gf*), Northern Gulf of Mexico (NGM), Southern Gulf of Mexico (SGM), Southern Pacific Slope (SPS), Huatulco (*hua*) and Chamela (*cha*); from now on, uppercase letters are used to identify regions that encompass more than one collection site (i.e., population), whereas

lowercase letters identify regions formed by a single collection site]. For the outgroup two alternatives geographical areas were defined: (A) South America (*C. luteicollis*, *C. smaragdulus*) and (B) Northwest Mexico, central, east and south U.S. (*C. viridis*).

### 3. Results

#### 3.1. Genetic structure and diversity

The length of the alignment obtained with the three loci was 2196 base pairs (*ITS2* = 667 bp, *16S* = 766 bp and *COI* = 763 bp) with a total of 76 haplotypes. The number of haplotypes per locus was nine for *ITS2*, 37 for *16S* and 66 for *COI* (Table 2). These sequences were uploaded in GenBank, and were registered under accession numbers from KX807611 to KX807722. Genetic diversity was slightly lower for *ITS2* ( $\pi = 0.0022$ ,  $Hd = 0.7306$ ) than for the mitochondrial loci ( $\pi = 0.0092$ ,  $Hd = 0.9547$  for *16S*;  $\pi = 0.0310$ ,  $Hd = 0.9850$  for *COI*). The  $Hd$  within regions containing more than one population varied with the marker analyzed. For *16S* all the  $Hd$  values were similar (NGM = 0.8, SGM = 0.828 and SPS = 0.81), but were heterogeneous for the others. The  $Hd$  values for *ITS2* were NGM = 0.3250, SGM = 0.2966 and SPS = 0.2667, whereas for *COI* were NGM = 0.6810, SGM = 0.9890 and SPS = 0.9810.

The SAMOVA of the combined data for  $K = 2$  to 6 population groups showed a gradual increase in the  $F_{CT}$  values. The optimal grouping was obtained for  $K = 6$  (i.e., *gf*, NGM, SGM, SPS, *hua* and *cha*; Table 3). Mantel test revealed a significant positive correlation between genetic and geographic distances ( $r = 0.396$ ,  $P = 0.0129$ ) suggesting isolation by distance.

The non-hierarchical AMOVA showed higher genetic structure for the nDNA (*ITS2*:  $F_{ST} = 0.89$ ), followed by the mtDNA loci (*16S*:  $F_{ST} = 0.74$ , *COI*:  $F_{ST} = 0.70$ ). In all the three loci most of the genetic variation is due to differences between the populations (*ITS2* 88.59%  $P < 0.0001$ , *16S* 74.37%  $P < 0.0001$ , *COI* 71.544%  $P < 0.0001$ ; Table 4A). The hierarchical

AMOVA, with the populations partitioned in regions (i.e., *gf*, NGM, SGM, SPS, *hua* and *cha*), showed that the genetic variation is due mainly to differences between regions (*ITS2* 83.75%  $P < 0.0001$ , *16S* 74.88%  $P < 0.0001$ , *COI* 71.54%  $P < 0.0001$ ) and, to a lesser extent, to differences between populations within regions (*ITS2* 5.95%  $P < 0.0001$ , *16S* 1.62%  $P < 0.0001$ , *COI* 1.37%  $P < 0.0001$ ; Table 4B).

The *ITS2* network comprises nine haplotypes interconnected by one to three mutational changes (Fig. 1A). Three haplogroups are recognized: haplogroup I, with six haplotypes, includes the individuals from SGM, SPS and *hua*. Haplogroup II has only one haplotype that includes the individuals from the *cha* population, and haplogroup III has two haplotypes including the *gf* population from the Eastern Sierra Madre and the populations from the NGM region. On the other hand, the network for *16S* recovers five haplogroups encompassing 37 haplotypes connected by up to 7 mutations (Fig. 1B); whereas the *COI* sequences form six haplogroups with 66 haplotypes interconnected by 1 to 16 mutational steps (Fig. 1C). Although the mitochondrial loci have higher haplotype diversity than the nuclear locus, the identified haplogroups show geographic consistency among the three genes. These haplogroups correspond with the grouping generated by the SAMOVA (i.e., *gf*, NGM, SGM, PSP, *hua* and *cha*; Table 2).

### 3.2. Genealogical reconstruction

The best-fit model of nucleotide substitution was HKY (nst=2) for the three loci; varying only in their specific parameters (*16S rRNA*: gamma = 0.175, p-inv = 0.358; *COI*: gamma = 1.417). The core of the genealogy recovered from the combined data matrix is a monophyletic clade (PP = 1) formed by *C. cyanellus* (Fig. 2). The first split shows six individuals from *gf* forming a well-supported clade (PP = 1), that is the sister group of the rest of the specimens. The next node includes the *cha* population as an independent group (PP = 0.94) that is sister to the clade

composed by the four remaining regions (NGM, *hua*, SPS and SGM). Within this clade, two monophyletic groups are recovered. Four individuals from *gf* plus all the individuals from NGM constitute the first one. The second group (PP = 0.81), designated as the "great lineage" henceforth, encompasses most of the morphological variation observed in *C. cyanellus*. This "great lineage" contains the southernmost populations on the distribution range of this species in Mexico. Within the "great lineage", the *hua* population forms a well-supported monophyletic clade (PP = 1), that is sister to the samples from SPS + SGM. Although the SGM region formed a well-supported monophyletic group (PP = 0.99), the individuals collected in the populations from the SPS region do not show reciprocal monophyly. The genealogies obtained from the individual analyses showed consistent topologies [supplementary material S1 (nDNA), and S2 (mtDNA)].

### 3.3. Divergence times and Historical demography

The chronogram (Fig. 3) inferred from the combined data set shows that the radiation of *C. cyanellus* occurred during the Pleistocene. The diversification events that gave origin to the main lineages within this species occurred in a time range of 1.63 to 0.91 Myr (nodes I to V). The Fu's  $F_s$  values were negative for the SGM+SPS+*hua* clade ( $F_s = -31.005$ ,  $P < 0.00001$ ) and for the NGM lineage ( $F_s = -4.749$ ,  $P < 0.01$ ). These negative values denote an increase in the effective population size ( $N_e$ ). By contrast, a reduction in the  $N_e$  for the *gf+cha* lineage was inferred ( $F_s = 4.986$ ,  $P = 0.028$ ); nonetheless, this might be the result of the deep divergence of the two subclades. The skyline plots show that the populations remained in stasis during most of the Pleistocene, followed by a period of demographic expansion towards the end of this epoch. For the "great lineage" the increment in  $N_e$  occurred ca. 180 000 years ago (Fig. 3A); whereas, for the NGM happened ca. 80 000 years ago (Fig. 3B). The *gf+cha* clade apparently suffered a slight

reduction in the  $N_e$ , which became more pronounced ca. 50 000 years ago, followed by a recovery ca. 20 000 years ago during the last glacial maximum (Fig. 3C).

### 3.4. Biogeographical scenario

The S-DIVA (Fig. 4) suggests a complex biogeographic scenario. The analysis infers at least 10 dispersal and 11 vicariant events during the evolutionary history of this species. Apparently, no historical migrations were detected between the north (*cha*, *gf*, *pap*, *tp*) and the south populations (*hua*, *jal*, *man*, *raye*, *tx*, *ver*). Alternative combinations of areas were recovered to represent the most probable ancestral distribution for *C. cyanellus* in Mexico (Fig. 4, node A); however, the areas *gf*, *cha* and *hua* recurrently were part of those combinations. For the internal nodes the analysis inferred better-defined scenarios with ancestral ranges restricted to combinations of high probability areas (e.g., SPS-SGM node B, SGM node C, SPS node D and *hua* node E).

## 4. Discussion

### 4.1. Genetic structure and diversity

The genetic diversity estimated in the present study with *ITS2* for *Canthon cyanellus* was lower compared to that estimated for the *16S rRNA* and *COI* loci. This difference is consistent with the fact that, in insects, mtDNA genes evolve faster than nDNA genes, particularly those coding for proteins (Andújar et al., 2016; Chung-Ping and Danforth, 2004; Timmermans et al., 2016). The differences in  $\pi$  and  $H_d$  between *C. cyanellus* and phytophagous beetles (Table 5) may be related to differences in life-history characteristics, dispersal strategies and body size, which determine gene flow and the effective population size (Kang et al., 2012). In the present study,  $H_d$  was consistently higher in the populations inhabiting transformed environments, than in those inhabiting preserved areas [(e.g., *tx* (grasslands) versus *cha* (deciduous tropical forest)]. These

results are related to the fact that *C. cyanellus* is more abundant in tropical fragmented landscapes than in preserved forests (Favila and Halffter 1997; Arellano et al 2008). We found, in particular, that the southernmost populations of the distribution range (i.e., *hua*, *jal*, *man*, *raye*, *tx* and *ver*) showed higher Hd than the populations at the Northern part (i.e., *cha*, *gf*, *pap* and *tp*). In addition, our results also show that *C. cyanellus* is a highly polymorphic species, given the large number of single haplotypes per population. Thus, the absence of haplotypes widely distributed across populations and geographical regions may be due to limited historical gene flow and to the fact that the populations current genetic structure has been determined by historical (isolation by distance) and contemporary (e.g., landscapes transformation) processes that restrict gene exchange between populations due to the fragmentation of landscapes as those existing in the Neotropic (Benitez-Malvido et al., 2016; Bandon et al., 2016; Fischer, 2007; Mock et al., 2007).

The phylogeographic structure of *C. cyanellus* is similar to that of other taxa with neotropical distribution in Mexico. Pringle et al. (2012) analyzed populations of ants of the genus *Azteca* (from Mexico to northern Nicaragua) and identified five lineages in *Azteca pittieri*, which differed genetically during the Pleistocene, two of them at the Pacific slope (i.e., Chamela and Huatulco). Suggesting limited historical gene flow between geographically separate populations. In contrast, other studies carried out with other neotropical taxa, observe a more complex phylogeographic structure associated with the main mountain systems of Mexico (Daza et al. 2009; Pedraza-Lara et al., 2015, Suárez-Atilano et al., 2014). Implying that the recent phylogeographic structure of those taxa is due to events that occurred during the Pleistocene.

#### 4.2. Biogeographical scenario and diversification times

The mutation rate of 2.3% per million years for mtDNA is an accepted data for calibrating molecular clocks in beetles (Papadopoulou et al., 2010). Even though we used a 0.85% rate for

the *ITS2*, it should be emphasized that there is no agreed-upon mutation rate as the length of this fragment is highly variable among taxa (Coleman, 2003). If the rates used do represent the evolutionary dynamics within these regions for the genome of *C. cyanellus*, then the divergence times indicate that this species arose by the end of the Pliocene, followed by a subsequent radiation during the Pleistocene (Fig. 3). Based on the recovered genealogy, a series of cladogenetic events seemingly took place in a North-South spatial sequence once the ancestor occupied the area in which this species currently ranges

The spatial and temporal variations in habitat availability might have modeled the genetic and geographic structure of the populations that we see today. *Canthon cyanellus* buries the resource in soft soils for nesting (Favila and Díaz, 1996). It is likely that the microhabitat characteristics prevailing in forest fragments during the Pleistocene, during the interglacial when temperatures became warmer (Gibbard et al., 2010), would have allowed these beetles to find favorable conditions to breed. Similarly, Ornelas et al. (2013), found a Pleistocene divergence between different taxa associated to cloud forests in Mexico. These authors suggest that the genetic differentiation of the study species can be explained by the forest dynamics as influenced by the Quaternary climatic fluctuations.

Some of the divergences identified in the present study seem to be associated to various magmatic episodes that occurred along the Trans-Mexican Volcanic Belt particularly in the Veracruz area. One of the largest volcanism pulses is represented by the lava flows that occurred ca. 1.5 Myr in the area of Poza Rica and Metlatoyuca (Ferrari et al., 2005). It is likely that such geological activity is related to the isolation between the NGM region and the "great lineage". The divergences occurred in the southernmost distribution range of this species may be associated to the displacement along the coastal zones that the vegetation in the Mexican lowlands underwent. Forests drifted to the south during the Pleistocene colder periods; then they



returned to the North during the warmer periods (Gómez-Pompa, 1973). This process might have promoted vicariant events as has been suggested for other taxa distributed within Mexico (Guevara-Chumacero et al., 2010; Maldonado-Sánchez et al., 2016; Ornelas et al., 2013; Suárez-Atilano et al., 2014). Finally, the discovery of four individuals collected at the *gf* population that are genetically more related to individuals at the NGM region than to the other *gf* samples provide evidence of contemporary migration.

#### 4.3. Historical demography

The skyline-plot analyses (Fig. 3) suggests that the demographic expansion were postglacial (~128,000-116,000 years before present, Muhs 2002) and occurred after the divergence of the main lineages. This suggests that glacial and interglacial cycles could have had a major effect on the genetic diversity of those populations located at the Northern end of the distribution. Ruiz et al. (2010) identified demographic expansions in populations of *Dendroctonus pseudotsugae* located in the Mexican Sierra Madre Occidental, the Northwest U.S. and Southwest of Canada, but did not detect expansions in the Mexican Sierra Madre Oriental or the Southwest U.S. These authors suggest that the expansions occurred from the middle to the end of the Pleistocene, probably after a bottleneck caused by the glacial cycles. In contrast, our results do not point out to bottlenecks in any of the main lineages during the evolutionary history of *C. cyanellus*.

#### 4.5. Taxonomic considerations

The genetics of *Canthon cyanellus cyanellus* had been previously studied using RAPDs (Ortiz-Domínguez et al., 2010); however, no genetic structure was found in the Gulf of Mexico populations. Ortiz-Domínguez et al., (2006) however, based on cuticle hydrocarbons used for sexual recognition, suggest that allopatric populations may be undergoing an incipient speciation

process. The combined data set recovered five well supported ( $PP > 0.94$ ) monophyletic lineages (i.e., *gf*, NGM, SGM + SPS, *hua* and *cha*), which could be risen to the species level. However, these monophyletic clades do not correspond with the allocation of the subspecies (*sensu* Halffter, 1961); nor do they, necessarily represent a single phylogenetic species as suggested by Solís and Kolhman (2002). It is possible that different genetic and environmental factors determine the chromatic polymorphism of *Canthon cyanellus* (Favila et al., 2000), as has been observed in other beetles (Davis et al., 2008; Scholtz, 2009; Whitman and Agrawal, 2009). Additional studies on behavior, morphology and ecological niche can reinforce the results hereby obtained. Nevertheless, our data points out the need to review the taxonomic status and delimitation of the potential species that comprise the *C. cyanellus* complex.

#### 4.6. Conclusions

The phylogeographic analysis of the *Canthon cyanellus* complex in the Mexican Transition Zone indicates that this species diversified into five lineages during the Pleistocene, when the main mountain systems had already been formed. The lineages correspond to allopatric populations or groups of populations geographically separated. The cladogenesis can be associated with geological events (e.g. volcanic activity) and cycles of contraction and expansion of forests associated with Pleistocene climatic oscillations. These conclusions, however, must be considered as preliminary due to the lack of precise evolutionary rates for the different genes, along with the uncertainty observed in the phylogenetic reconstructions. This research is part of an ongoing effort for understanding the evolutionary history of beetles along the Mexican Transition Zone. Within this line, follow up studies of the genetic structure of Central and South American populations will help us to reach a robust taxonomic delimitation of the lineages here found in the *Canthon cyanellus* complex.

**Acknowledgments**

We are grateful to Eduardo Chamé, Alfonso Díaz-Rojas, Yemitzel Camarero Arellano, Ana María Soto Portilla and Jorge Blanco for their assistance in the field. To Cristina Bárcenas for her technical support in the sequencing work during the first phase of the project. We thank Rosa Ana Sánchez Guillen and Gonzálo Halffter Salas for their critical review of a previous version of this manuscript. This study was supported by CONACYT grant CB-168373.

ACCEPTED MANUSCRIPT

**References**

- Anducho-Reyes, M., Cognato, A.I., Hayes, J.L., Zuñiga, G., 2008. Phylogeography of the bark beetle *Dendroctonus mexicanus* Hopkins (Coleoptera: Curculionidae: Scolytinae). *Mol. Phylogenet. Evol.* 49, 930–940 <http://dx.doi.org/10.1016/j.ympev.2008.09.005>.
- Andújar C., Faille A., Pérez-González S., Zaballos J.P., Vogler A.P., Ribera I., 2016. Gondwanian relicts and oceanic dispersal in a cosmopolitan radiation of euedaphic ground beetles. *Mol. Phylogenet. Evol.* 99, 235-46. <http://dx.doi.org/10.1016/j.ympev.2016.03.013>.
- Alfaro, M.E., Huelsenbeck, J.P., 2006. Comparative performance of Bayesian and AIC-based measures of phylogenetic model uncertainty. *Syst. Biol.* 55, 89–96. <http://dx.doi.org/10.1080/10635150500433565>.
- Arellano, L., León-Cortés, J., Ovaskainen, O., 2008. Patterns of abundance and movement in relation to landscape structure: a study of a common scarab (*Canthon cyanellus cyanellus*) in Southern Mexico. *Landscape Ecology.* 23, 69–78. <http://dx.doi.org/10.1007/s10980-007-9165-8>.
- Bandelt, H.J., Forster, P., Röhl, A., 1999. Median-joining networks for inferring intraspecific phylogenies. *Mol. Biol. Evol.* 16, 37–48.
- Beebe, N.W., Saul, A., 1995. Discrimination of all members of the *Anopheles punctulatus* complex by polymerase chain reaction-restriction fragment length polymorphism analysis. *Am. J. Trop. Med. Hyg.* 53, 478–481.
- Benítez-Malvido, J., Dáttilo, W., Martínez-Falcón, A.P., Durán-Barrón, C., Valenzuela, J., López, S., Lombera, R., 2016. The multiple impacts of tropical forest fragmentation on arthropod biodiversity and on their patterns of interactions with host plants. *Plos One* 11, e0146461. <http://dx.doi.org/10.1371/journal.pone.0146461>

Blandón, A.C., Perelman, S.B., Ramírez, M., López, A., Javier, O., Robbins, C.S., 2016.

Temporal bird community dynamics are strongly affected by landscape fragmentation in a Central American tropical forest region. *Biodivers. Conserv.* 25, 311-330.

<http://dx.doi.org/10.1007/s10531-016-1049-2>.

Breeschoten, T., Doorenweerd, C., Tarasov, S., Vogler, A.P., 2016. Phylogenetics and biogeography of the dung beetle genus *Onthophagus* inferred from mitochondrial genomes. *Mol. Phylogen. Evol.* 105, 86-95.

<http://dx.doi.org/10.1016/j.ympev.2016.08.016>

Caccone, A., Amato, G.D., Powell, J.R., 1988. Rates and patterns of scnDNA and mtDNA divergence within the *Drosophila melanogaster* Subgroup. *Genetics.* 118, 671–685.

Coleman, A.W., 2003. ITS2 is a double-edged tool for eukaryote evolutionary comparisons.

*TRENDS in Genetics.* 19, 370–375. [http://dx.doi.org/10.1016/S0168-9525\(03\)00118-5](http://dx.doi.org/10.1016/S0168-9525(03)00118-5).

Chessel, D., Dufour, A.B., Thioulouse, J., 2004. The ade4 package I One-table methods. *R News.* 4, 5–10.

Chung-Ping, L., Danforth, B.N., 2004. How do insect nuclear and mitochondrial gene substitution patterns differ? Insights from Bayesian analyzes of combined datasets. *Mol. Phylogenet. Evol.* 30, 686–702. [http://dx.doi.org/10.1016/S1055-7903\(03\)00241-0](http://dx.doi.org/10.1016/S1055-7903(03)00241-0).

Davis, A.L.V., Brink, D.J., Sholtz, C.H., Prinsloo, L.C., Deschodt, C.M., 2008. Functional implications of temperature-correlated color polymorphism in an iridescent, scarabaeine dung beetle. *Ecol. Entomol.* 33, 771–779. <http://dx.doi.org/10.1111/j.1365-2311.2008.01033.x>.

Davis A, Frolov A, Scholtz C., 2008. The African dung beetle genera. Pretoria (South Africa): Protea Book House.

- Daza, JM., Smith, EN., Páez, VP., Parkinson, CL. 2009. Complex evolution in the Neotropics: The origin and diversification of the widespread genus *Leptodeira* (Serpentes: Colubridae). *Mol. Phylogen. Evol.* 53, 653–667.  
<http://dx.doi.org/10.1016/j.ympev.2009.07.022>.
- De la Mora, M., Piñero, D., Nuñez-Farfan, J., 2015. Phylogeography of specialist weevil *Trichobaris sonor*: a seed predator of *Datura stramonium*. *Genetica* 143, 681–691.  
<http://dx.doi.org/10.1007/s10709-015-9886-x>.
- De Queiroz, K., 2007. Species concepts and species delimitation. *Syst. Biol.* 56, 879–886.  
<http://dx.doi.org/10.1080/10635150701701083>.
- Dupanloup, I.S., Schneider, S., Excoffier, L., 2002. A simulated annealing approach to define the genetic structure of populations. *Mol. Ecol.* 11, 2571–2581.
- Drummond, A.J. Suchard, M.A., Xie, D., Rambaut, A., 2012. Bayesian phylogenetics with BEAUti and BEAST 1.7. *Mol. Biol. Evol.* 29, 1969–1973.  
<http://dx.doi.org/10.1093/molbev/mss075>.
- Excoffier, L., Lischer, H.E.L., 2010. Arlequin suit ver 3.5: A new series of programs to perform population genetics analyses under Linux and Windows. *Mol. Ecol. Res.* 10, 564–567.  
<http://dx.doi.org/10.1111/j.1755-0998.2010.02847.x>.
- Excoffier, L., Smouse, P., Quattro, J.M., 1992. Analysis of molecular variance inferred from metric distances among DNA restriction data. *Genetics.* 131, 479–491.
- Favila, M.E, Díaz, A., 1997. Escarabajos coprófagos y necrófagos. In: González-Soriano, E., Dirzo, R., Voght, R. (Eds.), *Historia Natural de Los Tuxtlas*. Universidad Nacional Autónoma de México, México D.F., México, pp 383–384.
- Favila, M.E., Díaz, A., 1996. *Canthon cyanellus cyanellus* LeConte (Coleoptera: Scarabaeidae) makes a nest in the field with several brood balls. *Coleopt. Bull.* 50, 52–60.

- Favila, M.E., Ruíz-Lizarraga, G., Nolasco, J., 2000. Inheritance of a red cuticular color mutation in the scarab beetle *Canthon cyanellus cyanellus* LeConte (Coleoptera: Scarabaeidae). *Coleopt. Bull* 54, 541–545. <http://dx.doi.org/10.1649/0010-065X>.
- Ferrari, L., Tagami, T., Eguchi M., Orozco-Esquivel, M.T., Petrone, C.M., Jacobo-Albarrán, J., López-Martínez, M., 2005. Geology, geochronology and tectonic setting of late Cenozoic volcanism along the Southwestern Gulf of Mexico: The Eastern Alkaline Province revisited. *J. Vol. Geoth. Res.* 146, 284–306. <http://dx.doi.org/10.1016/j.jvolgeores.2005.02.004>.
- Fischer J., Lindemayer, D.B., 2007. Landscape modification and habitat fragmentation: a synthesis. *Global Ecol. Biogeogr.* 16, 265–280. <http://dx.doi.org/10.1111/j.1466-8238.2007.00287.x>.
- Fu, Y.X., 1997. Statistical tests of neutrality of mutations against population growth, hitchhiking and background selection. *Genetics.* 147, 915–925.
- Gibbard, P.L., Head, M.J., Walker, M.J.C., 2010. Formal ratification of the Quaternary System/Period and the Pleistocene Series/Epoch with a base at 2.58 Ma. *J. Quaternary Sci.* 25, 96–102. <http://dx.doi.org/10.1002/jqs.1338>.
- Gómez-Pompa, A., 1973. Ecology of the vegetation of Veracruz. In: Graham, A. (Eds.), *Vegetation and vegetational history of northern Latin America*. Elsevier Publishing Company, Amsterdam, Netherlands, pp. 73–148.
- Guevara-Chumacero, L.M., López-Wilchis, R., Pedroche, F.F., Juste, J., Ibáñez, C., Barriga-Sosa, I.D.L.A., 2010. Molecular phylogeography of *Pteronotus davyi* (Chiroptera: Mormoopidae) in Mexico. *J. Mamm.* 91, 220–232. <http://dx.doi.org/10.1644/08-MAMM-A-212R3.1>.

- Hall, T.A., 1999. BioEdit: to user-friendly biological sequence alignment editor and analysis program for Windows 95/98/NT. Nucleic Acids Symp. Ser. 41, 95–98. Haldane, J.B.S., 1922. Sex ratio and unisexual sterility in hybrid animals. J. Genet. 12, 101–109. <http://dx.doi.org/10.1007/BF02983075>.
- Halffter, G., 1961. Monografía de las especies norteamericanas del género *Canthon* Hoffsg. (Coleop., Scarab.). Ciencia 20, 225–320.
- Halffter, G., 1976. Distribución de los insectos en la Zona de Transición Mexicana. Folia Entomol. Mex. 35, 1–64.
- Halffter, G., 1987. Biogeography of the montane entomofauna of Mexico and Central America. Ann. Rev. Entomol. 32, 95–114.
- Halffter, G., Martínez, A., 1977. Revisión monográfica de los *Canthonina* americanos. Parte IV. Clave para géneros y subgéneros. Folia Entomol. Mex. 38, 29–107.
- Kang, A.R., Baek, J.Y., Lee, S.H., Cho, Y.S., Kim, W.S., Han, Y.S., Kim, I., 2012. Geographic homogeneity and high gene flow of the pear psylla, *Cacopsylla pyricola* (Hemiptera: Psyllidae), detected by mitochondrial COI gene and nuclear ribosomal internal transcribed spacer 2. Anim. Cells Syst. 16, 145–153. <http://dx.doi.org/10.1080/19768354.2011.607511>.
- Kohlmann, B., Halffter, G., 1990. Reconstruction of a specific example of insect invasion waves: the cladistic analysis of *Canthon* (Coleoptera: Scarabaeidae) and related genera in North America. Quaest. Entomol. 26, 1–20.
- Kumar, S., Stecher, G., Tamura, K., 2016. MEGA7: Molecular Evolutionary Genetics Analysis Version 7.0 for bigger datasets. Mol. Biol. Evol. 33, 1870–1874. <http://dx.doi.org/10.1093/molbev/msw054>.



- Leaché, A.D., Palacios, J.A., Minin, V.N., Bryson Jr, R.W., 2013. Phylogeography of the Trans-Volcanic bunchgrass lizard (*Sceloporus bicanthalis*) across the highlands of south-eastern Mexico. *Biol. J. Linn. Soc.* 110, 852–865. <http://dx.doi.org/10.1111/bij.12172>.
- Librado, P., Rozas, J., 2009. DnaSP v5: a software for comprehensive analysis of DNA polymorphism data. *Bioinformatics.* 25, 1451–1452. <http://dx.doi.org/10.1093/bioinformatics/btp187>.
- Madison, W.P., Madison, D.R., 2010. Mesquite: a modular system for evolutionary analysis. Version 2.73 (online). <http://mesquiteproject.org>
- Maldonado-Sánchez, D., Gutiérrez-Rodríguez, C., Ornelas, J.F., 2016. Genetic divergence in the common bush-tanager *Chlorospingus ophthalmicus* (Aves: Emberizidae) throughout Mexican cloud forests: The role of geography, ecology and Pleistocene climatic fluctuations. *Mol. Phylogenet. Evol.* 99, 76–88. <http://dx.doi.org/10.1016/j.ympev.2016.03.014>.
- Mantel, N., 1967. The detection of disease clustering and a generalized regression approach. *Cancer Res.* 27, 209–220.
- Miller, M.A., Pfeiffer, W., Schwartz, T., 2010. Creating the CIPRES Science Gateway for inference of large phylogenetic trees. In *Proceedings of the Gateway Computing Environments Workshop (GCE)*, New Orleans, LA, pp. 1–8.
- Mock, K.E., Bentz, B.J., O’Neill, E.M., Chong, J.P., Orwin, J., Pfrender, M.E., 2007. Landscape-scale genetic variation in a forest outbreak species, the mountain pine beetle (*Dendroctonus ponderosae*). *Mol. Ecol.* 16:553–568. <http://dx.doi.org/10.1111/j.1365-294X.2006.03158.x>.

- Morrone J.J., 2015. Halffter's Mexican transition zone (1962–2014), cenocrons and evolutionary biogeography. *J. Zoolog. Syst. Evol. Res.* 53, 249–257.  
<http://dx.doi.org/10.1111/jzs.12098>.
- Mush, D.R., 2002. Evidence for the timing and duration of the last interglacial period from high-precision Uranium-Series Ages of corals on tectonically stable coastlines. *Quaternary Res.* 58, 36–40. <http://dx.doi.org/10.1006/qres.2002.2339>.
- Nei, M., 1987. *Molecular evolutionary genetics*. Columbia University Press, New York.
- Nylander, J.A.A., Olsson, U., Alström, P., Sanmartín, I., 2008. Accounting for phylogenetic uncertainty in biogeography: a Bayesian approach to dispersal-vicariance analysis of the thrushes (Aves: *Turdus*). *Syst. Biol.* 57, 257–268.  
<http://dx.doi.org/10.1080/10635150802044003>.
- Ornelas, J.F., Sosa, V., Soltis, D.E., Daza, J.M., González, C. Soltis, P.S., Gutiérrez-Rodríguez, C., Espinosa de los Monteros, A., Castoe, T.A., Bell, C., Ruiz-Sánchez, E., 2013. Comparative phylogeographic analyzes illustrate the complex evolutionary history of threatened cloud forests of northern Mesoamerica. *Plos One.* 8, e53283.  
<http://dx.doi.org/10.1371/journal.pone.0056283>.
- Ortiz-Domínguez, M., Favila-Castillo, M.E., González, D., Zuñiga, D., 2010. Genetic differences in populations of the ball roller scarab *Canthon cyanellus cyanellus* (Coleoptera: Scarabaeidae): a preliminary analysis. *Elytron.* 24, 99–106.
- Ortiz-Domínguez, M., Favila-Castillo, M., Mendoza-López, R., 2006. Mate recognition differences among allopatric populations of the Scarab *Canthon cyanellus cyanellus* (Coleoptera: Scarabaeidae). *Ann. Entomol. Soc. Am.* 99, 1248–1256.  
[http://dx.doi.org/10.1603/0013-8746\(2006\)99\[1248:MRDAAP\]2.0.CO;2](http://dx.doi.org/10.1603/0013-8746(2006)99[1248:MRDAAP]2.0.CO;2).

- Papadopoulou, A., Anastasiou, I., Vogler, A.P., 2010. Revisiting the insect mitochondrial molecular clock: The Mid-Aegean Trench calibration. *Mol. Biol. Evol.* 27, 1659–1672. <http://dx.doi.org/10.1093/molbev/msq051>.
- Pedraza-Lara C., Barrientos-Lozano, L., Rocha-Sánchez, A.Y., Zaldivar-Riveron, A., 2015. Montane and coastal species diversification in the economically important Mexican grasshopper genus *Sphenarium* (Orthoptera: Pyrgomorphidae). *Molecular Phylogenetics and Evolution* 84, 220–231. <http://dx.doi.org/10.1016/j.ympev.2015.01.001>.
- Pfeiler, E., Johnson, S., Polihronakis, R.M., Markow, T.A., 2013. Population genetics and phylogenetics relationships of beetles (Coleoptera: Histeridae and Staphylinidae) from the Sonoran Desert associated with rotting columnar cacti. *Mol. Phylogenet. Evol.* 69, 491–501. <http://dx.doi.org/10.1016/j.ympev.2013.07.030>.
- Posada, D., 2008. jModelTest: phylogenetic model averaging. *Mol. Biol. Evol.* 25, 1253–1256. <http://dx.doi.org/10.1093/molbev/msn083>.
- Pringle, E.G., Ramírez, S.R., Bonebrake, T.C., Gordon, D.M., Dirzo, R., 2012. Diversification and phylogeographic structure in widespread *Azteca* plants-ants from the northern neotropics. *Mol. Ecol.* 21, 3576–3592. <http://dx.doi.org/10.1111/j.1365-294X.2012.05618.x>.
- Rambaut, A., 2008. Fig Tree ver. 1.3.1. Edinburgh: Institute of Evolutionary Biology, University of Edinburgh. <http://tree.bio.ed.ac.uk/software/figtree/>
- Rambaut, A., Suchard, M.A., Xie, D., Drummond, A.J., 2014. Tracer v1.6. Available from <http://beast.bio.ed.ac.uk/Tracer>
- Robinson, M., 1948. A review of the species of *Canthon* inhabiting the United States (Scarabaeidae: Coleoptera). *Trans. Am. Entomol. Soc.* 74, 83–100.

- Ronquist, F., Teslenko, M., van der Mark, P., Ayres, D.L., Darling, A., Höhna, S., Larget, B., Liu, L., Suchard, M.A., Huelsenbeck, J.P., 2012. MrBayes 3.2: efficient Bayesian phylogenetic inference and model choice across a large model space. *Syst. Biol.* 61, 539–542.  
<http://dx.doi.org/10.1093/sysbio/sys029>.
- Ruiz, E.A., Rinehart, J.E., Hayes, J.L., Zuñiga, G., 2010. Historical demography and phylogeography of a specialist bark beetle, *Dendroctonus pseudotsugae* Hopkins (Curculionidae: Scolytinae). *Environ. Entomol.* 39, 1685–1697.  
<http://dx.doi.org/10.1603/EN09339>.
- Ruiz, E. A., Rinehart, J.E., Hayes, J.L., Zuñiga, G., 2009. Effect of geographic isolation on genetic differentiation in *Dendroctonus pseudotsugae* (Coleoptera: Curculionidae). *Hereditas.* 146, 79–92. <http://dx.doi.org/10.1111/j.1601-5223.2009.02095.x>.
- Sánchez-Sánchez, H., López-Barrera, G., Peñaloza-Ramírez, J.M, Rocha-Ramírez, V., Oyama, K., 2012. Phylogeography reveals routes of colonization of the bark beetle *Dendroctonus approximatus* Dietz in Mexico. *J. Hered.* 5, 638–650.  
<http://dx.doi.org/10.1093/jhered/ess043>.
- Simon, C., Frati, F., Beckenbach, A., Crespi, B., Liu, H., Flook, P., 1994. Evolution, weighting, and phylogenetic utility of mitochondrial gene sequences and a compilation of conserved polymerase chain reaction primers. *Ann. Entomol. Soc. Am.* 87, 651–701.  
<http://dx.doi.org/10.1093/aesa/87.6.651>.
- Solís, A., Kohlmann, B., 2002. El género *Canthon* en Costa Rica. *G. Ital. Entomol.* 10, 1–68.
- Scholtz, C.H., 2009. Environmental influence on the development of color. In: Scholtz, C.H., Davis, A.L.V., Kryger, U. (Eds.), *Evolutionary Biology and Conservation of dung beetles*. Pensoft, Sofia, Bulgarias, pp. 147–154.

- Suárez-Atilano, M., Burbrink F., Vázquez-Domínguez, E., 2014. Phylogeographical structure within *Boa constrictor imperator* across the lowlands and mountains of Central America and Mexico. *J. Biogeogr.* 41, 2371–2384. <http://dx.doi.org/10.1111/jbi.12372>.
- Tarasov, S., Génier, F., 2015. Innovative Bayesian and parsimony phylogeny of dung beetles (Coleoptera, Scarabaeidae, Scarabaeinae) enhanced by ontology-based partitioning of morphological characters. *PLoS ONE* 10, e0116671. <http://dx.doi.org/10.1371/journal.pone.0116671>.
- Timmermans, M.J.T.N., Barton, C., Haran, J., Ahrens, D., Culverwell, C.L., Ollikainen, A., Dodsworth, S., Foster, P.G., Bocak, L., Vogler, A.P., 2016. Family-Level Sampling of Mitochondrial Genomes in Coleoptera: Compositional Heterogeneity and Phylogenetics. *Genome Biol. Evol.* 8, 161–175. <http://dx.doi.org/10.1093/gbe/evv241>.
- Whitman, D.W., Agrawal, A.A., 2009. Phenotypic Plasticity of insects: Mechanism and consequences. In: Whitman, D.W., Ananthakrishnan, T.N. (Eds.), *What is phenotypic plasticity and why is it important?* Science Publishers Enfield, NH, USA, pp. 1–63.
- Yu, Y., Harris, A.J., Blair, C., He, X.J., 2013. RASP (reconstruct ancient state in phylogenies) 2.1 beta. <http://mnh.scu.edu.cn/soft/blog/RASP>.
- Yu, Y., Harris, A.J., He X., 2010. S-DIVA (Statistical Dispersal-Vicariance Analysis): A tool for inferring biogeographic histories. *Mol. Phylogenet. Evol.* 56, 848–850. <http://dx.doi.org/10.1016/j.ympev.2010.04.011>.

**Table 1**

List of the populations of *Canthon cyanellus* used in this study. Elevation is given in meters above sea level.

State /locality (code)	Location	Elevation	Vegetation
Tamaulipas, Gómez-Farías ( <i>gf</i> )	23.04801, -99.14334	379	Semi-deciduous tropical forest.
Veracruz, Tuxpan ( <i>tp</i> )	20.95444, -97.46611	52	Rain-fed permanent agriculture.
Veracruz, Papantla ( <i>pap</i> )	20.41667, -97.45000	200	Secondary herbaceous vegetation derived from evergreen tropical forest.
Veracruz, La Mancha ( <i>man</i> )	19.56881, -96.40924	194	Rain-fed annual and semi-permanent agriculture.
Veracruz, Jalcomulco ( <i>jal</i> )	19.32861, -96.74694	370	Rain-fed annual and permanent agriculture.
Veracruz, Los Tuxtlas ( <i>tx</i> )	18.58333, -95.06667	120	Secondary vegetation derived from evergreen tropical forest and grasslands.
Chiapas, Raymundo Enríquez ( <i>raye</i> )	14.86420, -92.30055	99	Rain-fed permanent agriculture.
Chiapas, El Vergel ( <i>ver</i> )	14.70294, -92.26723	22	Rain-fed annual agriculture.
Oaxaca, Huatulco ( <i>hua</i> )	15.78000, -96.09000	30	Mid-stature deciduous tropical forest.
Jalisco, Chamela ( <i>cha</i> )	19.49971, -105.0229	90	Low-stature deciduous tropical forest.

**Table 2**

Molecular diversity indices for each locus by population and region..

Region/population	<i>ITS2</i>	<i>16S</i>	<i>COI</i>	<i>ITS2</i>	<i>16S</i>	<i>COI</i>	<i>ITS2</i>	<i>16S</i>	<i>COI</i>	<i>ITS2</i>	<i>16S</i>	<i>COI</i>
	n	n	n	H	H	H	$\pi$	$\pi$	$\pi$	Hd	Hd	Hd
<i>gf</i>												
Tamaulipas, Gómez-Farías	10	10	10	2	4	6	0.0005	0.0084	0.0237	0.3556	0.6440	0.7780
NGM												
Veracruz, Tuxpan ( <i>tp</i> )	10	10	8	1	5	4	0.0000	0.0015	0.0058	0.0000	0.8000	0.7500
Veracruz, Papantla ( <i>pap</i> )	6	6	6	2	3	3	0.0009	0.0012	0.0054	0.60000	0.7330	0.6000
NGM total	16	16	14	2	6	6	0.0005	0.0016	0.0056	0.3250	0.8000	0.6810
SGM												
Veracruz, La Mancha ( <i>man</i> )	10	10	10	1	4	10	0.0000	0.0012	0.0127	0.0000	0.7110	10000
Veracruz, Jalcomulco ( <i>jal</i> )	10	10	10	2	6	10	0.0003	0.0020	0.0139	0.2000	0.8670	10000
Veracruz, Los Tuxtlas ( <i>tx</i> )	10	10	10	2	6	6	0.0000	0.0034	0.0107	0.5333	0.8440	0.8890
SGM total	30	30	30	3	12	26	0.0001	0.0025	0.0131	0.29660	0.8280	0.9890
SPS												
Chiapas, Raymundo Enríquez ( <i>raye</i> )	11	11	11	3	5	9	0.0006	0.0016	0.0114	0.3450	0.7820	0.9640
Chiapas, El Vergel ( <i>ver</i> )	10	10	10	2	5	9	0.0003	0.0015	0.0068	0.2000	0.7560	0.9780
SPS total	21	21	21	3	7	17	0.0004	0.0016	0.0091	0.2667	0.8100	0.9810
<i>hua</i>												
Oaxaca, Huatulco	8	10	9	1	8	7	0.0000	0.0028	0.0030	0.0000	0.9556	0.9170
<i>cha</i>												
Chamela, Jalisco	10	10	10	1	4	4	0.0000	0.0011	0.0011	0.0000	0.5330	0.6440
Global	95	97	94	9	37	66	0.0022	0.0092	0.0310	0.6740	0.9547	0.9850

n: Sample size; H: number of haplotypes;  $\pi$ : nucleotide diversity; Hd: haplotype diversity

**Table 3**

Fixation Index ( $F_{CT}$ ) for the population groups computed from the SAMOVA based on the combined data set (*ITS2*, *16S*, *COI*) in populations of *Canthon cyanellus*.

Population groupings	K	$F_{CT}$	P
( <i>gf</i> , <i>tp</i> , <i>pap</i> , <i>cha</i> ) ( <i>jal</i> , <i>man</i> , <i>tx</i> , <i>raye</i> , <i>ver</i> , <i>hua</i> )	2	0.408	< 0.01
( <i>gf</i> , <i>tp</i> , <i>pap</i> ) ( <i>jal</i> , <i>man</i> , <i>tx</i> , <i>raye</i> , <i>ver</i> ) ( <i>hua</i> , <i>cha</i> )	3	0.508	< 0.01
( <i>gf</i> , <i>tp</i> , <i>pap</i> ) ( <i>jal</i> , <i>man</i> , <i>tx</i> , <i>raye</i> , <i>ver</i> ) ( <i>hua</i> ) ( <i>cha</i> )	4	0.607	< 0.00001
( <i>gf</i> ) ( <i>tp</i> , <i>pap</i> ) ( <i>jal</i> , <i>man</i> , <i>tx</i> , <i>raye</i> , <i>ver</i> ) ( <i>hua</i> ) ( <i>cha</i> )	5	0.654	< 0.00001
( <i>gf</i> ) ( <i>tp</i> , <i>pap</i> ) ( <i>jal</i> , <i>man</i> , <i>tx</i> ) ( <i>raye</i> , <i>ver</i> ) ( <i>hua</i> ) ( <i>cha</i> )	6	0.728	< 0.001

*gf*: Gómez-Farías; *tp*: Tuxpan; *pap*: Papantla; *jal*: Jalcomulco; *man*: La Mancha; *tx*: Los Tuxtlas; *raye*: Raymundo Enríquez; *ver*: El Vergel; *hua*: Huatulco; *cha*: Chamela



**Table 4**

Analysis of molecular variance (AMOVA) for the nDNA locus (*ITS2*) and the mtDNA loci (*16S* and *COI*) in populations of *Canthon cyanellus*. (A) non-hierarchical AMOVA and (B) between geographical groups. \*  $P < 0.05$ .

	<i>ITS2</i>					<i>16S</i>					<i>COI</i>				
	df	SS	Est. Var.	Var. (%)		df	SS	Est. var.	Var. (%)		df	SS	Est. var.	Var. (%)	
A)															
BP	9	109.95	1.27	88.59	$F_{ST} = 0.89^*$	9	253.70	2.81	74.37	$F_{ST} = 0.74^*$	9	787.07	8.93	70.46	$F_{ST} = 0.70^*$
WP	85	13.92	0.16	11.41		87	84.32	0.97	25.63		84	314.28	3.74	29.54	
Total	94	123.87	1.44			96	338.01	3.78			93	1101.35	12.67		
B)															
BR	5	105.71	1.33	83.75	$F_{CT} = 0.84^*$	5	247.28	3.09	74.88	$F_{CT} = 0.75^*$	5	765.05	9.88	71.54	$F_{CT} = 0.72^*$
BPWR	4	4.25	0.09	5.95	$F_{ST} = 0.90^*$	4	6.42	0.07	1.62	$F_{ST} = 0.77^*$	4	22.01	0.19	1.37	$F_{ST} = 0.73^*$
WP	85	13.92	0.16	10.30	$F_{SC} = 0.37^*$	87	84.32	0.97	23.50	$F_{SC} = 0.06^*$	84	314.28	3.74	27.10	$F_{SC} = 0.05^*$
Total	94	123.87	1.59			96	338.01	4.12			93	1101.35	13.81		

BP: between populations; WP: within populations; BR: between geographic regions; BPWR: between populations within geographic regions

**Table 5**

Phylogeography studies conducted in Mexico for beetles.

Species	Area	N	Loci/bp	Hd	$\pi$	F <sub>ST</sub>	DE	Reference
<i>Belonuchus sp.</i>	Mexico	5	<i>COI</i> (mtDNA)/614	0.9540	0.0135	0.35	Yes	Pfeiler et al., 2013
<i>Iliotona beyeri</i>	Mexico	6	<i>16S</i> (mtDNA)/427	0.6200	0.0017	0.12	Yes	Pfeiler et al., 2013
			<i>COI</i> (mtDNA)/625	0.4420	0.0010	0.38		
<i>Carsinops gilensis</i>	Mexico	6	<i>16S</i> (mtDNA)/453	0.7580	0.0023	0.02	Yes	Pfeiler et al., 2013
			<i>COI</i> (mtDNA)/658	0.9330	0.0045	0.24		
<i>Canthon cyanellus</i>	Mexico	10	<i>ITS2</i> (nDNA)/667	0.6740	0.0023	0.89	Yes	This study
			<i>16S</i> (mtDNA)/766	0.9547	0.0092	0.74		
			<i>COI</i> (mtDNA)/763	0.9850	0.0310	0.70		
<i>Trichobaris soror</i>	Mexico	14	<i>COI</i> (mtDNA)/658	0.7220	0.0101	0.73	Yes	De la Mora et al., 2015
<i>Dendroctonus approximatus</i>	Mexico	15	<i>COI</i> (mtDNA)/492	0.8890	0.0171	0.48	Yes	Sánchez-Sánchez et al., 2012
<i>D. pseudotsugae</i>	Canada, USA and Mexico	17	<i>COI</i> (mtDNA)/550	0.9450	0.0270	0.80	NR	Ruiz et al., 2009
<i>D. mexicanus</i>	Mexico and Guatemala	25	<i>COI</i> (mtDNA)/246	0.8490	0.0154	0.85	Yes	Anducho-Reyes et al., 2008
<i>D. pseudotsugae</i>	Canada, USA and Mexico	34	<i>COI</i> (mtDNA)/550	0.982	0.0340	NR	Yes	Ruiz et al., 2010

N: Number of populations; Hd: haplotype diversity;  $\pi$ : nucleotide diversity; F<sub>ST</sub>: genetic differentiation; DE: demographic expansion; NR, value not reported

Figure legends

**Fig. 1.** Haplotype networks and distribution for the populations of *Canthon cyanellus* in Mexico. (A) *ITS2* nuclear gene, (B) *16S rRNA*, and (C) *COI* mitochondrial genes. The Roman numeral indicates the respective haplogroup, the size of the pie is proportional to the haplotype frequency, whereas the number is the amount of samples having that haplotype in that particular locality (if the pie has no number, that haplotype is a singleton). The studied populations are located in the map with specific colors corresponding to the haplotype networks. The Mexican mountain systems are highlighted by contour lines corresponding to Sierra Madre Occidental (grey), Sierra Madre Oriental (brown), Trans-Mexican Volcanic Belt (black), Sierra Madre del Sur (green), Sierra Madre de Chiapas (yellow), Central Highlands of Chiapas (purple) and the Isthmus of Tehuantepec (red line).

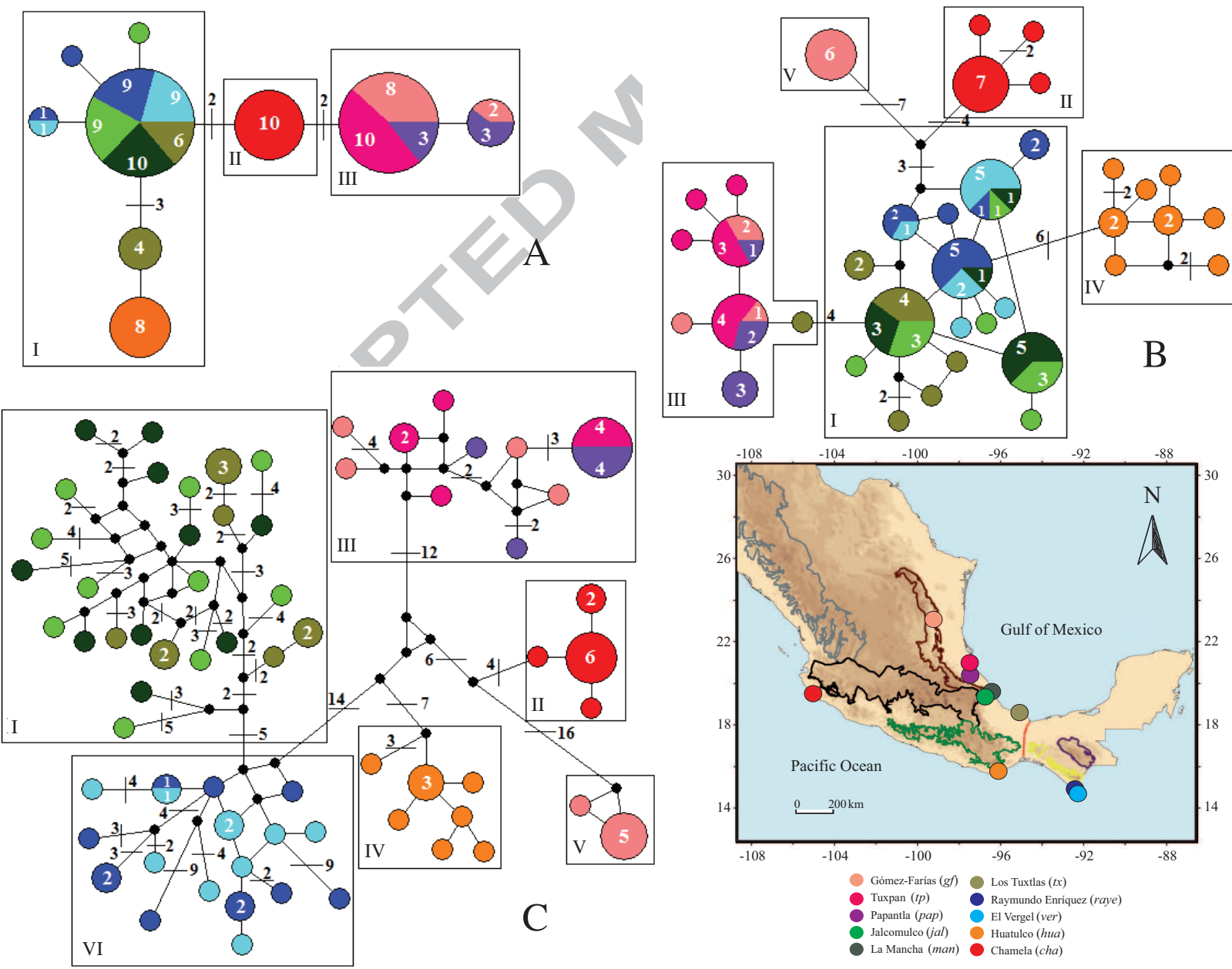
**Fig. 2.** Consensus tree obtained for the combined data set (*ITS2*, *16S* and *COI*) based on a Bayesian inference analysis. The individuals are indicated with the same color used in Fig 1 to identify their population of origin. The numbers indicate Bayesian posterior probabilities. NGM: Northern Gulf of Mexico, *cha*: Chamela, *hua*: Huatulco, SPS: Southern Pacific Slope, SGM: Southern Gulf of Mexico, and *gf*: Gómez-Farías. The different morphs found in the respective geographic regions are shown.

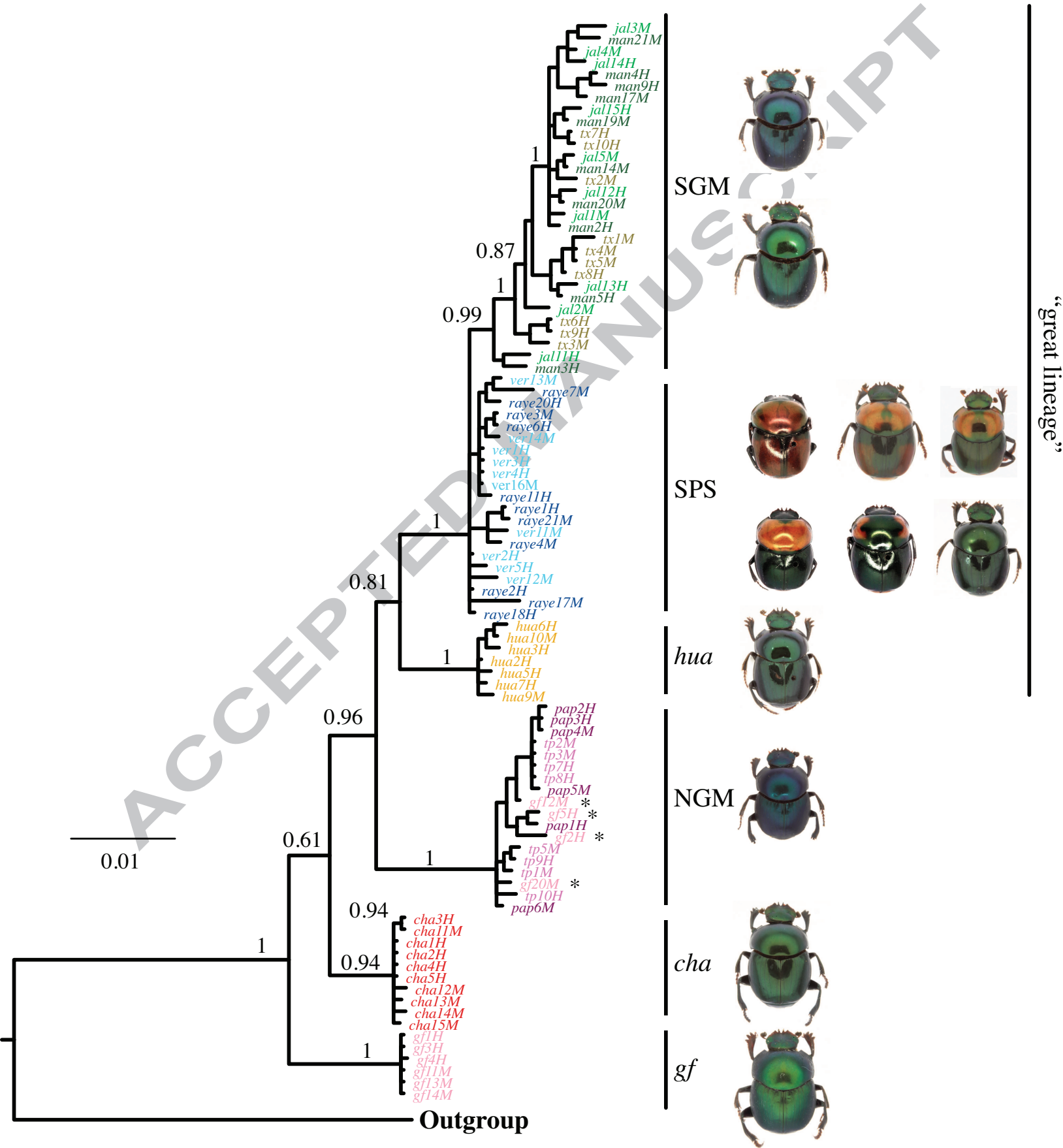
**Fig. 3.** Chronogram inferred from BEAST analysis and demographic history for the major clades. Time is given in millions of years. Nodes with posterior probabilities above 0.9 show time uncertainty by means of 95% HPD bars. Skyland plots display the historical demographic tendency of the mayor lineages. The red line indicates the trend of the median  $N_e$ ; whereas the blue lines represent the 95% confidence limits. (A) “Great lineage” demographic trend ( $F_u$ ’s  $F_s$  =

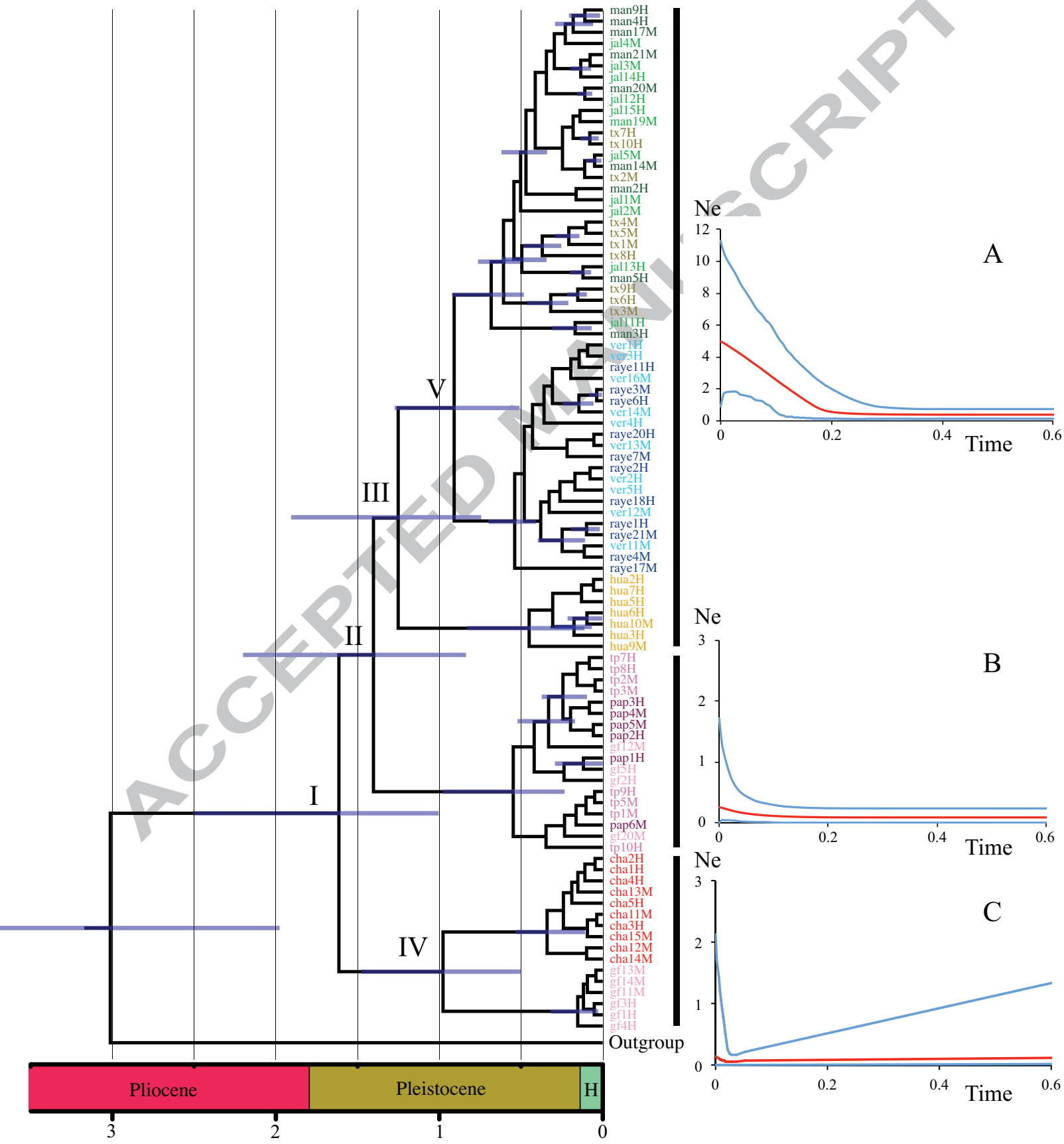
-31.01,  $P < 0.0001$ ), (B) Skyland plot for the NGM geographic region (Fu's  $F_s = -4.75$ ,  $P < 0.01$ ), and (C) Demographic history for the *gf-cha* lineage (Fu's  $F_s = 4.99$ ,  $P < 0.01$ ).

**Fig. 4.** Biogeographical scenario (dispersal-vicariance) plot on a condensed tree assembled from 79,996 trees obtained in during the BEAST analysis. The numbers indicate the marginal probability for each hypothetical ancestral range, only values  $> 80\%$  are shown.

ACCEPTED MANUSCRIPT

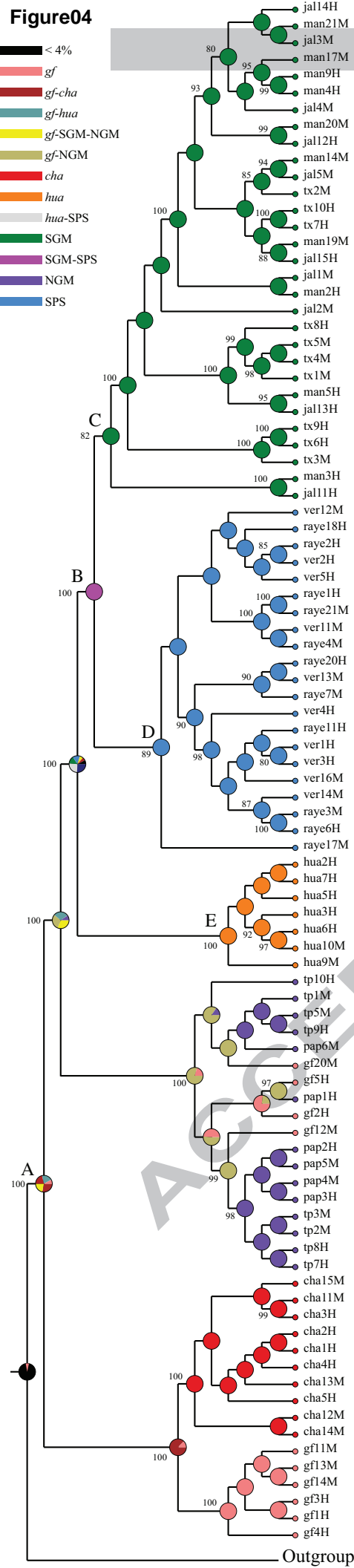




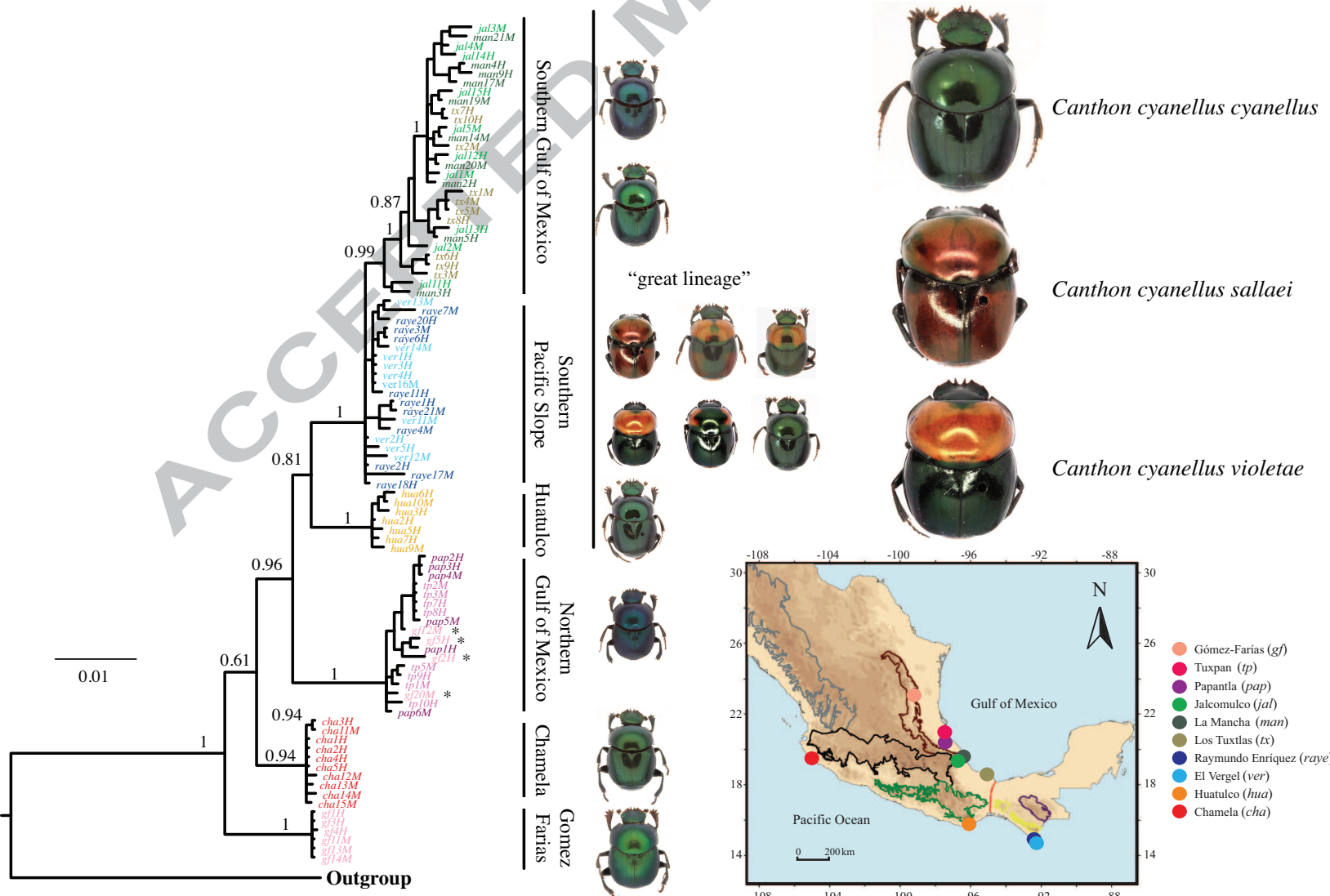


**Figure04**

ACCEPTED MANUSCRIPT







- Phylogeographic analyses of *Canthon cyanellus* in Mexico reveals lineages historical differentiation.
- The divergence of this Neotropical group occurred during the Pleistocene.
- Geological events and glacial cycles influenced the geographic structure of the lineages.
- The demographic history suggests post-glacial expansions.
- Not all the current valid subspecies are supported by the molecular analysis.

ACCEPTED MANUSCRIPT